4th International Conference on Molten Slags and Fluxes, 1992, Sendai, ISIJ

CALCULATION OF PHASE DIAGRAMS FOR OXIDE SLAGS BY THERMODYNAMIC MODELS

Wataru Yamada and Tooru Matsumiya

Advanced Materials & Technology Research Labs., Nippon Steel Corp., Japan

Synopsis: Binary and multi-component phase diagrams of ZrO_2-bearing oxide slags and refractories were calculated by the use of thermodynamic model. In the calculation, the activities of oxide components in molten slags were estimated by CELL MODEL for molten slag. The interaction energies among the oxide components in molten slags were estimated based on the experimentally observed phase diagrams of the binary systems. The calculated results are be presented in the systems, ZrO_2-SiO_2-CaO-Al_2O_3, which are important in considering the reactions between refractories and slags.

Key words: Phase Diagrams Thermodynamics Zirconia Refractory Slag

1. Introduction

Refining slags sometimes erode the refractory materials of container of molten steel in refining process. It makes the strength of the container weak and serious impurities enter into slags and affects the refining reactions. In order to prevent such reactions, it is necessary to understand the phase diagrams of oxide phase diagrams. In recent days, several thermodynamic models of oxide molten slags have been developed [1-3] and some phase diagrams of oxide systems have become to be able to be calculated.

For ZrO_2 bearing oxide systems, only a few works of the assessment [4,5] by the thermodynamic models were done, most of which are only valid to the binary systems and are difficult to be extended to multi-component systems. This is partially because such assessments are based on the simple regular solution model. On the other hand, quasi-chemical cell model [1] shows excellent representativity of thermodynamic quantities of multicomponent liquid oxides, only taking use of binary energy parameters. In the present study, cell model was adapted to the assessment of ZrO_2-A_xO_y(A:Si, Al, Mg, Ca, Fe) binary systems. And taking use of the binary energy parameters, the phase diagrams of ZrO_2-SiO_2-Al_2O_3 and ZrO_2-CaO-Al_2O_3 ternary systems are calculated.

2. Assessment procedure

For oxide systems, experimental data used in the assessment, are phase boundary data available in literature. The model parameters of the cell model [1] have been assessed by the use of the mainly liquidus temperature lines data. Assessed systems are as following binaries.

ZrO_2-SiO_2, Al_2O_3, FeO, MgO, CaO.

In cell model, cations are ordered in valence order [1] The valence of

zirconium ion in the liquid oxide mixture are considered as 4+, which is the same as that of Si. We put the cation Zr^{4+} after Si^{4+}. By the use of assessed parameters, whole or a part of phase diagrams have been calculated in order to evaluate the reasonability of calculated phase diagrams in comparison with the observed ones. In the calculation of phase diagrams, THERMO-CALC[6] was used.

3.Result

The results of the assessment of respective binary system is as follows.

SiO_2-ZrO_2

ZrO_2 transforms from tetragonal to cubic at 2250 ℃. However, during whole temperature range, standard free energies of liquid and solid ZrO_2 are described as a unique temperature function. This treatment does not affect the assessment so much because the change in heat capacities between cubic and tetra is not large. The phase diagrams for this system[7] has one monotectic and one eutectic reactions. Figure 1 shows the calculated activities of ZrO_2 and SiO_2 at 2270 ℃ with the optimized parameter values. The calculated activity curves well represent the liquid miscibility gap at intermediate composition range. Optimized parameters have to be given a slight composition dependence, which will be discussed later together with parameter values for other oxide systems. Calculated phase diagram is shown in figure 2.

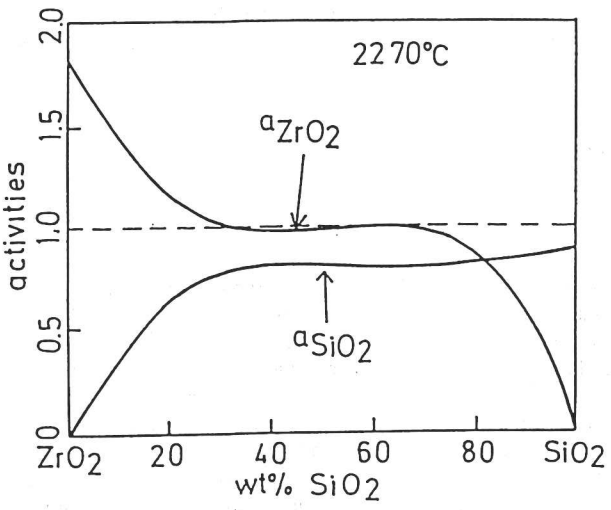

Fig. 1 Calculated activities of ZrO_2 and SiO_2 at 2270°C. Standard states are pure solid ZrO2 and SiO_2, respectively

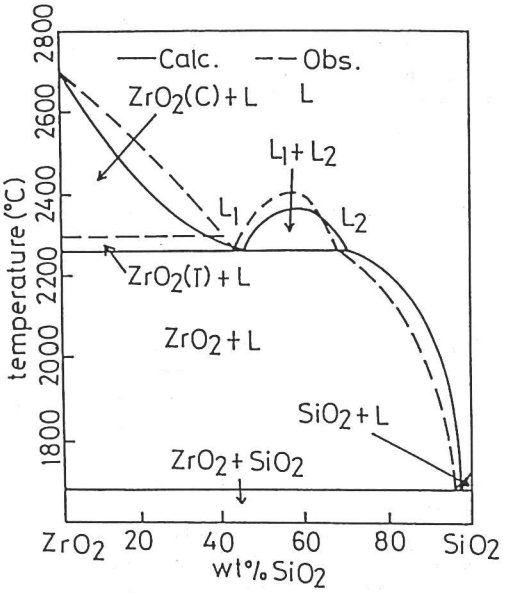

Fig. 2 Calculated and observed[7] phase diagram for ZrO_2-SiO_2 sysrtem

Al_2O_3-ZrO_2

In the phase diagrams of Al_2O_3-ZrO_2 system, ε-Al_2O_3 phase was observed near pure Al_2O_3 composition[8]. We neglected the existence of this phase because the thermodynamic functions for this phase is not known. In the assessment procedure, attention was mainly paid to the composition and the temperature of the eutectic point (44%ZrO_2, 1710°C in figure 3) and liquidus temperature in equilibrium with ZrO_2. The optimized phase diagram by cell model is in good agreement with the observed one except for the discrepancy of liquidus line near pure Al_2O_3. This discrepancy came from our ignoring the existence of ε-Al_2O_3.

FeO-ZrO_2

In this system, phase diagram has one eutectic point (2.8%ZrO_2, 1336°C)[9]. Parameter optimization was made by representing observed eutectic point and compositions dependence of liquidus temperature in equilibrium with ZrO_2. In this case, the formation energy parameter mainly determines

the position of eutectic point and interaction energy parameter determined temperature dependence of liquidus line. The optimized diagram (figure 4) shows a slight discrepancy with regard to the eutectic temperature and composition. However we cannot discuss the validity of the model from this discrepancy because of the lack of the precision of observed data.

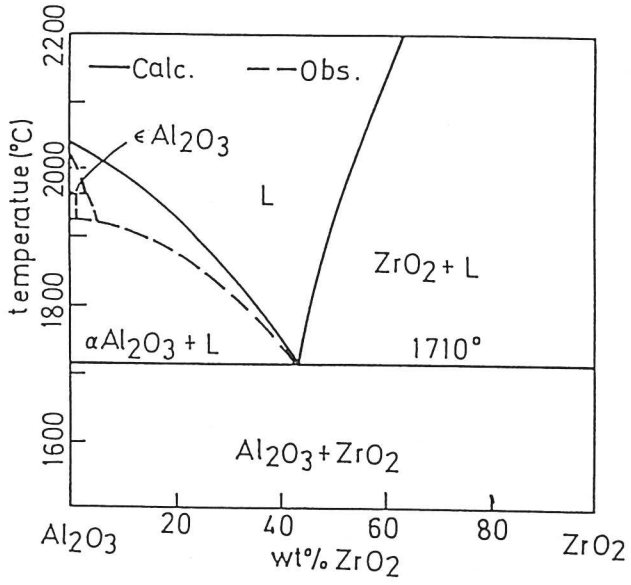

Fig. 3 Calculated and observed[8] phase diagram for Al2O3-ZrO2 system.

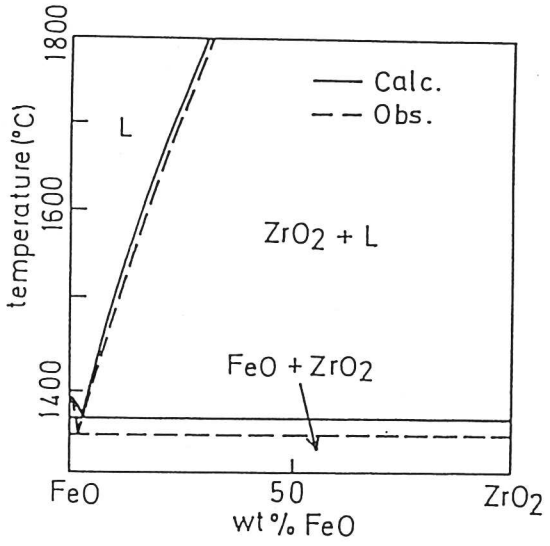

Fig. 4 Calculated and observed[9] phase diagram for FeO-ZrO2 system.

MgO-ZrO_2

In this system, whole phase diagram is not available. Only liquidus lines were observed[10] as shown in figure 5. The diagram suggests the existence of binary compound which has congruent melting point around 12%MgO. However, such a compound has not been reported to exist in other literature and thermodynamic functions were not known. Therefore we neglected the existence of the compound. In addition, another phase diagram indicates the wide composition range of miscibility gap in cubic-ZrO_2 up to 22% MgO. We also neglected the miscibility gap in the assessment of model parameters. Parameter optimization was made based on the data of eutectic point (50%MgO, 2113°C) and liquidus lines. Calculated phase diagram represented the location of eutectic point but could not represent the upward concave liquidus line in equilibrium with MgO. We gave up doing further assessment because it seemed to meaningless in the situation where details of the equilibrium phases and reliability of observed data in this region are not well known.

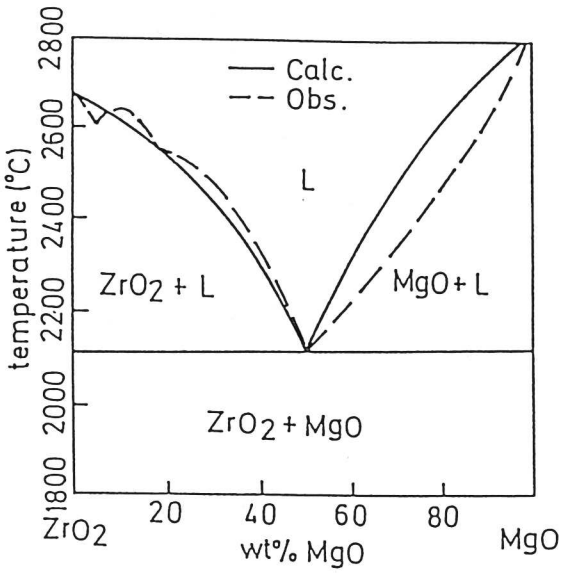

Fig. 5 Calculated and observed[10] phase diagrm for ZrO2-MgO system

CaO-ZrO_2

We could not find CaO-ZrO_2 binary phase diagrams. We collected the observed equilibrium phase sets from the phase diagram for CaO-SiO_2-ZrO_2 ternary system as shown in figure 6[11]. All information we can get from this

figure are that there are two eutectic point at the both side of the binary compound $CaO \cdot ZrO_2$ (which might have congruent melting point) in $CaO-ZrO_2$ binary phase diagrams. One of them is located at $50\%ZrO_2$, 2260^oC (No.1) and the other at $77\%ZrO_2$, 2285^oC (No.2). Regardless such a poor information, we tried to assess the model parameters for this system because CaO is very important species in ZrO_2 bearing slags or nonmetallic inclusions. We could not find the formation energy value of CaOZrO2 compound, either. During the assessment, the existence of ZrO_2 solid solution was ignored and ZrO_2 is assumed as pure oxide. Optimization of the phase diagram were done as following procedure. First the model parameters were optimized as calculated activity of CaO becomes unity at the eutectic point No.1 and activity of ZrO2 becomes unity at eutectic point No.2. The calculated activities and formation energies of $CaO \cdot ZrO_2$ compound at eutectic points with optimized parameters are tabulated in table 1, where the formation energies $\triangle G$'s were calculated by the equation,

$$\triangle G_{CaO \cdot ZrO} = RT \ln (a_{CaO} * a_{ZrO_2}).$$

Table 1 Calculated activities and formation energies of $CaO \cdot ZrO_2$ at eutectic points

eutectic point	temperature (^oC)	wt%ZrO_2	aCaO	aZrO_2	$\triangle G_{CaO\text{-}ZrO_2}$ (cal/mol)
No1	2260	50.1	1.0	0.56	-3340
No2	2285	77	0.52	1.0	-2911

The formation energies are assumed to have linear temperature dependence and was given by the use of the table values, as -46800+17.2T (cal/mol). Optimized phase diagram was shown in figure 7.

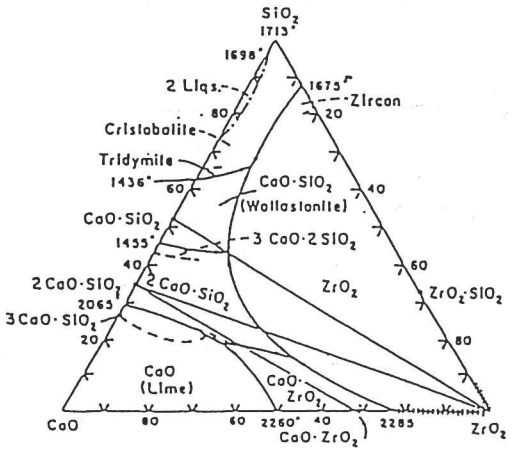

Fig. 6 Observed phase diagram[11] for $CaO-SiO_2-ZrO_2$ system.

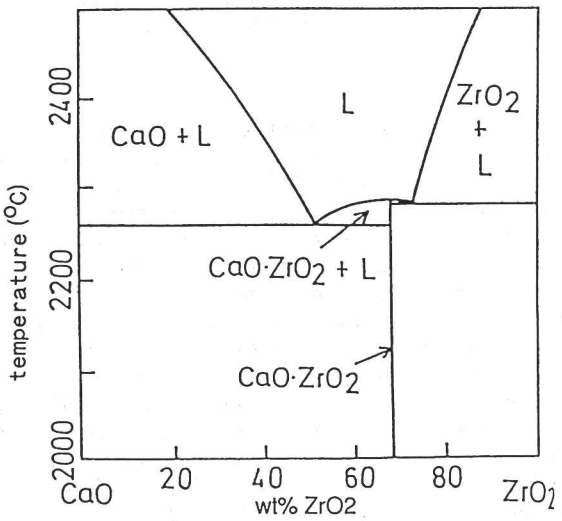

Fig. 7 Calculated phase diagram for $CaO-ZrO_2$ system.

4. Discussions

4.1 Interpretation of assessed parameter values

Optimized parameter values are summarized in table 2. In the system of ZrO_2-SiO_2, tendency of formation of liquid miscibility gap in the phase diagrams are shown. The results of the present assessment indicated that the tendency can be represented by setting positive values as asymmetric cell's formation energies. Cell model can be adapted to these systems containing miscibility gap without introduction of any unnatural constraint. Furthermore, the parameters have only a slight composition dependence. As a whole, because of the shortage of observed data, the optimized parameters have a certain degree of ambiguity. Therefore, accumulation of precise observation data, especially activity data, are needed in order to estimate the validity of cell model to these oxide systems. However the roughly assessed binary parameters can predict the phase diagrams of ternary systems as shown in the following section.

Table 2 Energy parameters in cell model for ZrO_2

ZrO_2 system

i - j	W^O_{ij}(cal/mol)	E^O_{ij}(cal/mol)
SiO_2 - ZrO_2	$3000-1000X_{SiO2}$	500
ZrO_2 - Al_2O_3	-1900	3000
ZrO_2 - FeO	500	-2000
ZrO_2 - MnO	-	-
ZrO_2 - MgO	-1000	-2500
ZrO_2 - CaO	-1000	-5000

4.2 Estimation of ternary phase diagrams

By the use of the assessed parameter values obtaind by the present work, the phase diagrams for ZrO_2-SiO_2-Al_2O_3 and ZrO_2-CaO-Al_2O_3 were calculated. The calculated equi-liquidus temperature lines for ZrO_2-SiO_2-Al_2O_3 is shown in figure 8 together with the observed ones[12]. The agreement between the calculated phase diagram and the observed one becomes worse especially in $2SiO_2 \cdot 3Al_2O_3$ saturation region. In this region, it was pointed out that the cell model overestimates the stability of liquid oxide phase[1]. Further improvement in the cell model is necessary in this region. Figure 9 shows the calculated equi-liquidus temperature lines for ZrO_2-CaO-Al_2O_3. It is expected that the present calculation underestimated the stability of the liquid oxide phase because in the assessment of ZrO_2-CaO binary, the existence of ZrO_2 solid solution was ignored. In order to improve the precision of the model calculation, it is necessary to construct the thermodynamic model of the ZrO_2 solid solution in ZrO_2-CaO based refractory materials systems.

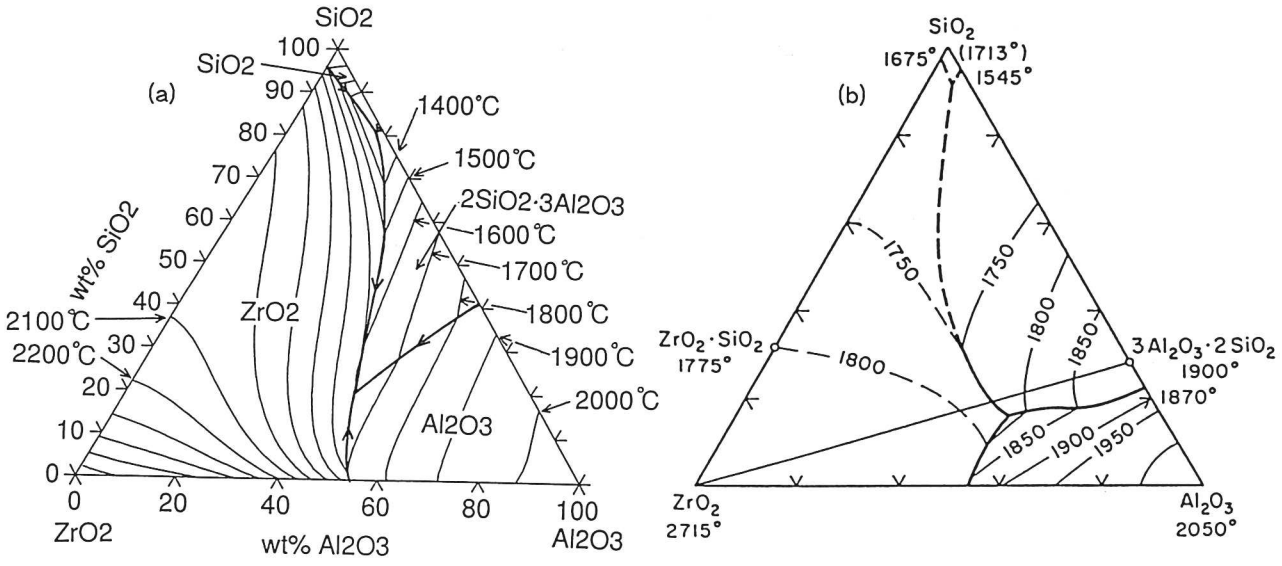

Fig. 8 Calculated (a) and observed (b)[12] phase diagram for ZrO_2-SiO_2-Al_2O_3.

5. Conclusion

Cell model was extended to the ZrO_2 bearing oxide systems. The assessed results are reasonable in that it can represent the binary phase diagrams without the unnatural

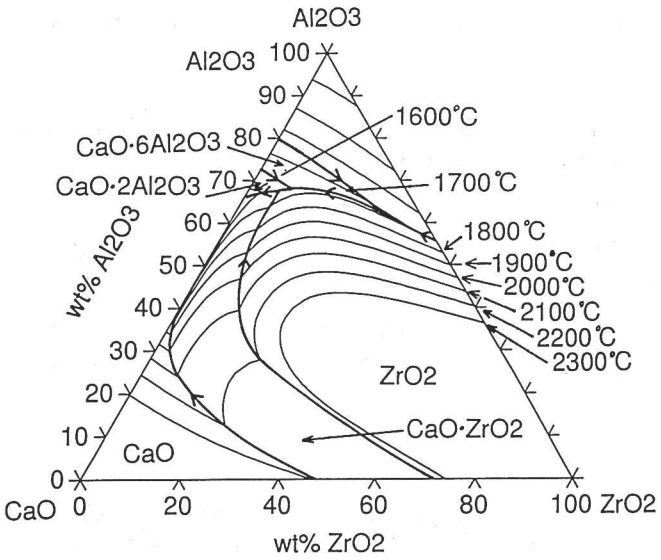

Fig. 9 Calculated phase digaram of $CaO-ZrO_2-Al_2O_3$

constraints in the model parameters in each binary system. However, some problems still exist in the phase diagram calculation of ternary systems. One of them is the wrong precision of the cell model in $2SiO_2 \cdot 3Al_2O_3$ saturation region and the other is the necessity of the thermodynamic modeling of the ZrO_2 solid solution.

REFERENCES

1)H.Gaye and J.Welfringer: Second Int. Symposium on Metallurgical Slags and Fluxes, The Metall. Soc. AIME, Wallendale, Pensylvania, (1984),357
2)J.Lumsden: Physical Chemistry of Process Metallurgy, Part I, Inter science Publisher, New Yprk, N.Y., (1961),165
3)M. Hillert, B. Jansson, B. Sundman and J. Agren: Met. Trans., 16A(1985),661
4)S.A.Degtyarev and G.F.Voronin: CALPHAD 12(1987),73
5)Y.Du and Z.Jin: CALPHAD 15(1991),59
6)B.Sundman, B.Jansson and J.-O.Andersson: CALPHAD 9(1985),52
7)W.C.Butterman and W.R.Foster: Am. Mineralogist 52(1985),153
8)G.Covales: Ber. Deut. Keram. Ges., 45(1968),217
9)W.A.Fischer and A.Hoffman: Arch. Eisenhuttenw., 28(1957)743
10)T.Noguchi and M.Nizuno:Bull. Chem. Soc. Jap., 41(1587),41
11)S.Koide: Asahi Garasu Kenkyu Houkoku, 4(1954),8
12)P.P.Badnikov and A.A.Lituakovskii:Daklady Akad. Nauk S.S.S.R., 106(1956),268